CONTRAST MEDIA & MOLECULAR IMAGING
*Contrast Med. Mol. Imaging* **1**: 15–22 (2006)
Published online 15 February 2006 in Wiley InterScience (www.interscience.wiley.com). DOI:10.1002/cmmi.87

CONTRAST MEDIA & MOLECULAR IMAGING

Full Paper

# Specific E-selectin targeting with a superparamagnetic MRI contrast agent

*Sébastien Boutry, Sophie Laurent, Luce Vander Elst and Robert N. Muller**

*Department of General, Organic and Biomedical Chemistry, NMR and Molecular Imaging Laboratory, University of Mons-Hainaut, B-7000 Mons, Belgium*

*Received 29 September 2005; Revised 30 November 2005; Accepted 1 December 2005*

ABSTRACT: Targeting of the endothelial inflammatory adhesion molecule E-selectin by magnetic resonance imaging (MRI) was performed with a superparamagnetic contrast agent in the context of *in vitro* and *in vivo* models of inflammation. The specific contrast agent was obtained by grafting a synthetic mimetic of sialyl Lewis$^x$ (sLe$^x$), a natural ligand of E-selectin expressed on leukocytes, on the dextran coating of ultrasmall particles of iron oxide (USPIO). This new contrast agent, called USPIO-g-sLe$^x$, was tested, *in vitro*, on cultured human umbilical vein endothelial cells (HUVECs) stimulated to express inflammatory adhesion molecules, and *in vivo*, on a mouse model of hepatitis. *In vitro*, HUVECs were stimulated with the pro-inflammatory cytokine tumor necrosis factor alpha (TNF-$\alpha$) and were then incubated with USPIO-g-sLe$^x$ or ungrafted USPIO. *In vivo*, hepatitis was induced on NMRI mice by injection of concanavalin A (Con A). USPIO-g-sLe$^x$ and ungrafted USPIO were injected intravenously. *In vitro* results showed an extensive retention of USPIO-g-sLe$^x$ on TNF-$\alpha$ stimulated HUVECs. Image intensity and $R_2$ measurements performed on $T_2$-weighted MR images demonstrated a significantly higher binding of USPIO-g-sLe$^x$ on stimulated HUVECs. *In vivo*, USPIO are known to pass through the fenestrae of the liver and to be captured by Kupffer cells, inducing a loss of signal intensity on $T_2$-weighted MR images. Unexpectedly, when injected to Con A-treated mice, USPIO-g-sLe$^x$ induced a significantly lower attenuation of liver signal intensity than USPIO or USPIO-g-sLe$^x$ injected to healthy mice, or USPIO injected to Con A-treated mice, suggesting that the specific contrast media is retained extracellularly by an interaction with E-selectin overexpressed on the vascular endothelium. Both *in vitro* and *in vivo* results therefore indicate that USPIO-g-sLe$^x$ is recognizing endothelial E-selectin. USPIO-g-sLe$^x$ is thus well suited for the MRI diagnosis of inflammation and for the *in vitro* evaluation of endothelial cells activation. Copyright © 2006 John Wiley & Sons, Ltd.

KEYWORDS: E-selectin; molecular MRI; contrast agent; sialyl-Lewis$^x$; iron oxide; endothelial cells; liver; inflammation

## INTRODUCTION

The noninvasive diagnosis and monitoring of inflammation processes are of particular relevance considering their involvement in a broad spectrum of pathologies, such as infection, rheumatoid arthritis, ischemia, graft rejection, atherosclerosis and formation of tumor metastasis (1–5). In this context, inflammatory cells, such as macrophages, can be tagged *in vivo* with ultrasmall particles of iron oxide (USPIO). Macrophages are indeed able to take up USPIO by phagocytosis, and to subsequently invade tissues through inflammatory processes. This has been achieved in a model of central nervous system (CNS) inflammation (6–8). In this rat model, microglial cells, which are the major intrinsic component of the CNS immune response, internalize USPIO and are detected by *in vivo* MRI (9, 10). However, this type of cellular MRI requires high doses of iron oxide nanoparticles to saturate the macrophages located in lymph nodes, liver, spleen or bone marrow. Labeling of macrophages with USPIO in atherosclerotic plaques has also been achieved (11). Lymphocytes themselves can be magnetically labeled *ex vivo* by fluid phase endocytosis of iron oxide nanoparticles and re-injected in the blood circulation for MRI studies of the *in vivo* trafficking (12). An alternative strategy to image inflammation is to

**Correspondence to:* R. N. Muller, Department of General, Organic and Biomedical Chemistry, NMR and Molecular Imaging Laboratory, University of Mons-Hainaut, B-7000 Mons, Belgium.
E-mail: robert.muller@umh.ac.be
*Contract/grant sponsor:* IUAP, Federal State of Belgium; contract/grant number: VP5/04.
*Contract/grant sponsor:* ARC Program, French Community of Belgium; contract/grant number: 00/05–258.

**Abbreviations used:** b.w., body weight; CNS, central nervous system; Con A, Concanavalin A; ECGS, endothelial cell growth supplement; FBS, fetal bovine serum; HBSS, Hank's balanced salt solution; HUVECs, human umbilical vein endothelial cells; i.p., intraperitoneal; MCDB 131, Molecular Cell and Developmental Biology medium 131; MR, mannose receptor; NMRD, nuclear magnetic resonance dispersion; PBS, phosphate buffer saline; SE, signal enhancement; SI, signal intensity; sLe$^x$, Sialyl-Lewis$^x$; SPIO, small particles of iron oxide; TNF-$\alpha$, tumor necrosis factor $\alpha$; USPIO, ultrasmall particles of iron oxide; USPIO-g-sLe$^x$, sLe$^x$ grafted to USPIO.

develop MRI contrast agents specifically targeting an inflammatory cellular marker like the endothelial adhesion molecules. For this molecular imaging purpose, high relaxivities and high specificity are necessary due to the limited number of targets. With Gd-based contrast agents, a huge number of paramagnetic centers are often needed to get to the adequate detection level (13). Owing to their large number of iron atoms, superparamagnetic nanoparticles of iron oxide have strong $T_2$ and $T_2^*$ effects and are therefore detectable at very low concentrations (14, 15). Their usefulness as markers in molecular imaging has been proven in studies on *in vitro* specific targeting of E-selectin (16).

E-selectin is a transmembrane adhesion glycoprotein expressed on the vascular endothelium during inflammation. Its natural ligand, the sialyl-Lewis$^x$ (sLe$^x$) [Fig. 1(a)] is expressed by leukocytes. The expression of inflammatory adhesion molecules can be transcriptionaly upregulated by cytokines, such as interleukin-1 (IL-1) or tumor necrosis factor $\alpha$ (TNF-$\alpha$). *In vitro*, E-selectin is expressed between 4 to 30 h after stimulation by IL-1 or TNF-$\alpha$, with a peak of expression at 6 h post-stimulation (17). In a previous work, the synthesis of a paramagnetic complex coupled to a mimetic of the sLe$^x$ molecule [Fig. 1(b)] has been described (18). The resulting specific contrast agent has been evaluated in different animal models of inflammation (19–21). Owing to their high payload of magnetic ions and subsequently to their very high 'particulate relaxivity', iron oxide nanoparticles are attractive reporters for molecular imaging. In the present study, the synthesis of a new specific superparamagnetic contrast agent, the USPIO-g-sLe$^x$, obtained by coupling the sLe$^x$ mimetic to USPIO is reported as well as the evaluation of its potential as MRI contrast agent, *in vitro* on human umbilical vein endothelial cells cultures stimulated by TNF-$\alpha$ and *in vivo* in a mouse model of hepatitis.

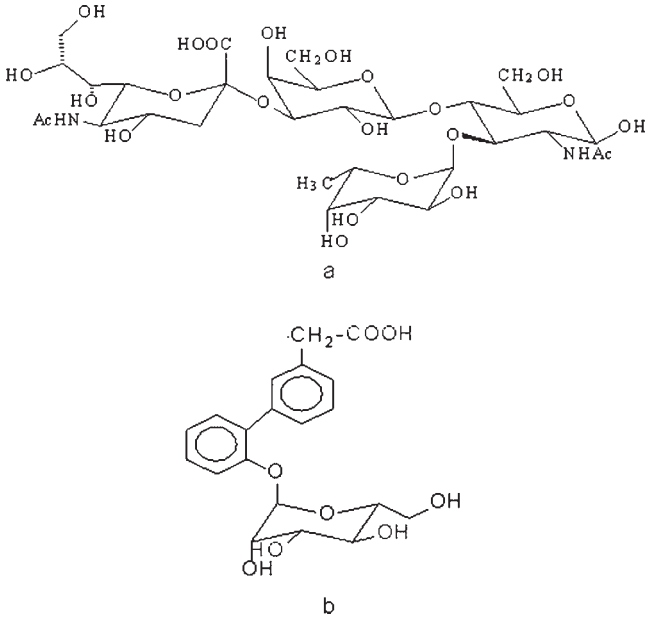


**Figure 1.** Structure of the sialyl-Lewis$^x$ (a) and of the mimetic molecule (b).

## MATERIALS AND METHODS

### Contrast agent

The USPIO used was a dextran-coated nanoparticle of iron oxide (crystal size 5–6 nm, overall size 20–40 nm) obtained by the classical Molday method (22). A mimetic of the sLe$^x$ molecule was synthesized as described (18) and branched to the dextran coating of the USPIO. The coupling between the sLe$^x$ mimetic and the nanoparticle coating was realized by a reaction involving epichlorhydrin and the aminated sLe$^x$ mimetic (Fig. 2). Aliquots of 2.5 ml of USPIO (50 mg Fe) were diluted in 10 ml of water and treated with 10 ml NaOH 5M and 5 ml of epichlorhydrin. The mixture was stirred for 24 h at 40 °C and dialyzed. A solution of sLe$^x$ mimetic (10 mg) in 2 ml of water was added to the USPIO–epichlorhydrin suspension (150 μmol Fe). The mixture was stirred overnight at room temperature and then dialyzed for 48 h (cut-off membrane 12 000–14 000).

### Relaxometry

The NMRD relaxation profiles were recorded from 10 kHz to 10 MHz on a STELAR field cycling relaxometer (Stelar, srl, Mede, Italy). Additional measurements at 20 and 60 MHz were performed on Bruker Minispec systems (Bruker, Karlsruhe, Germany).

### *In vitro* studies

Human umbilical vein endothelial cells (HUVECs) were provided by the Metastasis Research Laboratory of the University of Liège, Belgium (Professor V. Castronovo). HUVECs were cultured in 0.2% gelatin-coated 75 cm$^2$ culture dishes (Greiner, Wemmel, Belgium) using MCDB 131 medium (InvitroGen, Merelbeke, Belgium), supplemented with 20% fetal bovine serum (FBS, InvitroGen, Merelbeke, Belgium), 2 mM of L-glutamine (InvitroGen, Merelbeke, Belgium), 50 μg/ml of heparin (Aventis Pharma S.A., Brussels, Belgium) and 1% antibiotic—antimycotic solution (InvitroGen, Merelbeke, Belgium) (23). Endothelial cell growth supplement (ECGS) (Sigma-Aldrich, Bornem, Belgium) was prepared from the lyophilized powder (5 mg/ml in sterilized phosphate buffer saline, PBS) and added to the medium at a concentration of 50 μg/ml (10 μl/ml of medium). To stimulate the expression of E-selectin, cells were treated during 5 h with 10 ng/ml of the pro-inflammatory cytokine TNF-$\alpha$ (17). TNF-$\alpha$ (Alexis Biochemicals,

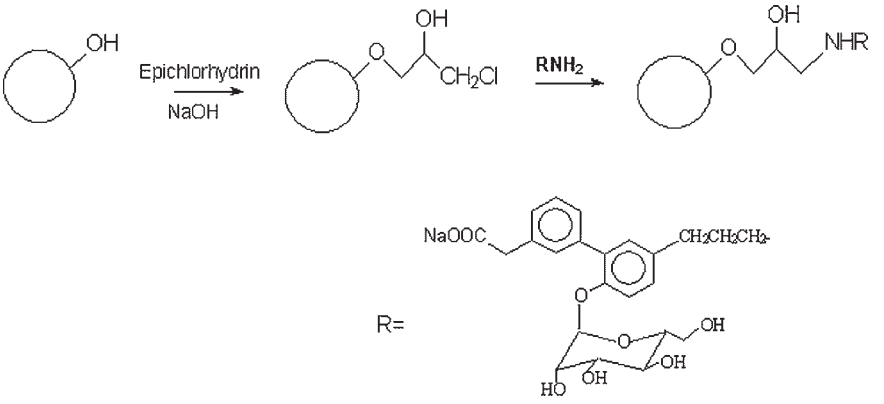


**Figure 2.** Synthesis of the USPIO-g-sLe$^x$.

Lausen, Switzerland) was prepared by dissolving the lyophilized powder in sterile demineralized water (10 μg/ml). This stock solution was then diluted in sterile PBS and brought to a concentration of 0.5 μg/ml. Stimulated and unstimulated cells were scraped 5 h after addition of TNF-$\alpha$, and were counted using a hemocytometer. After a 5 min centrifugation at 3000 rpm, cells were resuspended at $10^7$ cells/ml in complete medium and put in the wells of 96-well microculture plates (Greiner, Wemmel, Belgium) for the incubation with the contrast agents. USPIO or USPIO-g-sLe$^x$ were added to the cells to get a final iron concentration of 4 mM (total volume for the incubation was 200 μl). After 1 h of incubation, microculture plates were centrifugated during 10 min at 1000 rpm to remove unbound contrast agent. Then, cells were washed twice with 200 μl Hank's balanced salt solution (HBSS). After the second washing, cells were resuspended in 100 μl HBSS and transferred in 250 μl PCR tubes (Greiner, Wemmel, Belgium). PCR tubes were centrifugated for 5 min at 3000 rpm, the HBSS supernatant was removed and the cells were finally resuspended in 100 μl of 2% gelatin for MR imaging. The concentration of cells for MRI was $2 \times 10^7$ cells/ml.

### *In vivo* studies

All the animal experiments fulfill the requirements of the Ethical Committee of our institution. Hepatitis was induced on NMRI mice (25–35 g) by intravenous (tail vein) injection of 20 mg/kg of the plant lectin concanavalin A (Con A, from *Canavalia ensiformis*, Jack bean; Sigma-Aldrich, Bornem, Belgium). The animals were anesthetized with 50 mg/kg b.w., i.p. nembutal (Sanofi, Brussels, Belgium), and USPIO-g-sLe$^x$ was injected in the tail vein at a dose of 30 μmol Fe/kg to Con A-treated mice and to healthy mice used as controls. USPIO was also injected at the same dose to healthy and Con A-treated mice as nonspecific control. NMRI mice were provided by the Laboratory of Biology and Embryology of the University of Mons-Hainaut, Belgium (Professor H. Alexandre).

### MR imaging and data analysis

MR images were obtained on a Bruker AVANCE-200 system, equipped with a vertical 4.7 T magnet. For the *in vitro* studies, a $T_2$-weighted spin-echo sequence was used [*TR*/*TE* 3000/15 ms; 24 echo images (from 15 to 360 ms) recolted; FOV 4 cm; matrix 256 × 256; four acquisitions; acquisition time 28 min 36 s]. Paravision software was used to measure $T_2$ values and signal intensities on cell samples MR images. Relative signal intensity enhancement (SE) was calculated as a percentage of the signal intensity of samples containing non-incubated cells on the 150 ms echo image, using the following formula:

$$(SE) = 100 \times \frac{(SNR)_{incubated\ cells} - (SNR)_{non\text{-}incubated\ cells}}{(SNR)_{non\text{-}incubated\ cells}}$$

For the *in vivo* experiments, one pre-contrast and several post-contrast axial images of the liver were acquired at different delays (2–120 min) after the injection of the particles [2D gradient echo (GE) sequence; *TR*/*TE* 58.8/5.2 ms; FOV 5.5 cm; matrix 256 × 256; flip angle 50°]. Con A-treated mice were imaged 5 h after the induction of hepatitis. Paravision software was used to measure signal intensities (SI) of ROIs chosen in the liver parenchyma on MR images. Signal-to-noise ratio (SNR) was calculated and relative signal enhancement (SE) was obtained with the following formula:

$$(SE) = 100 \times \frac{(SNR)_{post\text{-}contrast} - (SNR)_{pre\text{-}contrast}}{(SNR)_{pre\text{-}contrast}}$$

Color maps were assigned to *in vivo* MR images using the OSIRIS software package.

## RESULTS AND DISCUSSION

### Relaxivity

The relaxivity profiles ($r_1$) of USPIO-g-sLe$^x$ and USPIO are represented in Fig. 3. $r_2$ values of USPIO-g-sLe$^x$ and USPIO at 20 MHz and 37 °C are, respectively, 75.5 and

 

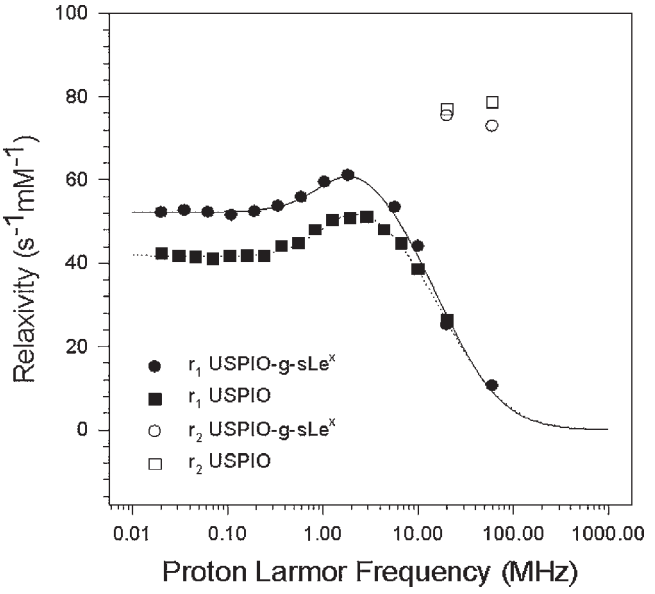


**Figure 3.** NMRD profiles ($r_1$) of USPIO-g-sLe$^x$ (•) and USPIO (■), and $r_2$ values (at 20 and 60 MHz) of USPIO-g-sLe$^x$ (○) and USPIO (□).

$77\,s^{-1}\,mM^{-1}$. At 60 MHz and 37 °C, these values are respectively 73 and $78.6\,s^{-1}\,mM^{-1}$ (Fig. 3). As compared with the parent particles, the branching of the synthetic mimetic of the sLe$^x$ molecule does not induce a major change of the relaxometric properties above 10 MHz (0.235 T).

## MR imaging *in vitro*

HUVECs were chosen because this cell type is able to express adhesion molecules such as selectins or molecules of the superfamily of immunoglobulins after stimulation by IL-1 or TNF-$\alpha$ (17). A $T_2$-weighted MR image of

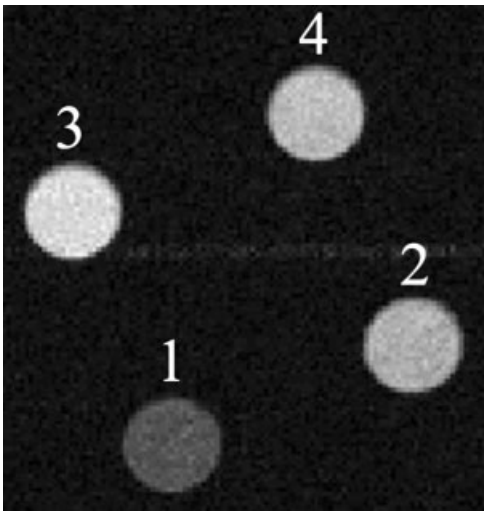


**Figure 4.** Axial spin echo $T_2$-weighted MR Image (TR/TE: 3000/15 ms, 24 echoes, FOV: 4 cm, matrix: $256 \times 256$) of PCR tubes containing HUVECs ($2 \times 10^7$ cells/ml in 2% gelatin). 1: TNF-$\alpha$ stimulated +4 mM USPIO-g-sLe$^x$, 2: unstimulated +4 mM USPIO-g-sLe$^x$, 3: TNF-$\alpha$ stimulated +4 mM ungrafted USPIO, 4: unstimulated +4 mM ungrafted USPIO. (Image at TE = 150 ms).

PCR tubes containing HUVECs resuspended in 2% gelatin, stimulated or not with TNF-$\alpha$ and after incubation with USPIO-g-sLe$^x$ or ungrafted USPIO, is shown in Fig. 4. The darkest signal corresponds to stimulated HUVECs after incubation with USPIO-g-sLe$^x$. Obviously, a larger amount of specifically targeted contrast agent interacts with stimulated HUVECs.

This is quantitatively confirmed by the signal intensities on $T_2$-weighted MR images which show that the largest negative enhancement occurs with USPIO-g-sLe$^x$ and TNF-$\alpha$ stimulated cells (Fig. 5). A slight decrease of signal is, however, observed in control groups. Endothe-

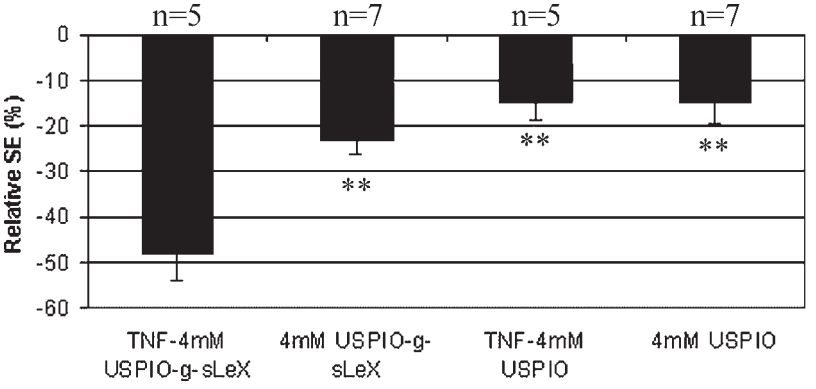


**Figure 5.** Analysis of signal intensities measured on MR images (TE = 150 ms) of TNF-α-stimulated and unstimulated HUVEC samples ($2 \times 10^7$ cells/ml), incubated with 4 mM USPIO-g-sLe$^x$ or ungratfted USPIO. Relative signal intensity enhancement of the different HUVEC samples are shown as a percentage of the signal intensity of non-incubated cells. The results are represented as averages ± SEM and were statistically processed using Student's *t*-test: **: $P < 0.01$ as compared to the TNF-$\alpha$-stimulated HUVEC samples incubated with 4 mM USPIO-g-sLe$^x$. (''n'' is the number of analyzed cell samples).

 

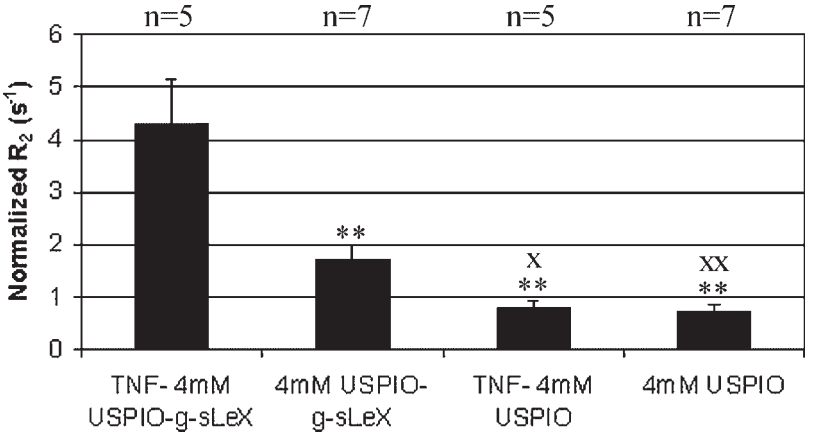


**Figure 6.** $R_2$ values of TNF-$\alpha$-stimulated and unstimulated HUVEC samples ($2 \times 10^7$ cells/ml), after an incubation with 4 mM USPIO-g-sLe$^x$ or ungrafted USPIO. Normalization of $R_2$ values was obtained by removing the $R_2$ of non-incubated cells. The results are represented as averages $\pm$ SEM and were statistically processed using Student's *t*-test: **: $P < 0.01$ as compared to the TNF-$\alpha$-stimulated HUVEC samples incubated with 4 mM USPIO-g-sLe$^x$, xx: $P < 0.01$ and x: $P < 0.05$ as compared to the unstimulated HUVEC samples incubated with 4 mM USPIO-g-sLe$^x$. (''n'' is the number of analyzed cell samples).

lial cells, which are part of the reticulo-endothelial system, are indeed able to nonspecifically capture USPIO or USPIO-g-sLe$^x$ by macropinocytosis (24). As expected, the larger $r_2$ effect is induced by the USPIO-g-sLe$^x$ on TNF-$\alpha$-treated HUVECs, confirming that these stimulated cells are retaining more specific USPIO than unstimulated HUVECs (Fig. 6). The $r_2$ value of the latter ones incubated with USPIO-g-sLe$^x$ significantly differs from the values obtained from HUVECs, stimulated or not, and incubated with ungrafted USPIO. In the case of unstimulated HUVECs incubated with USPIO-g-sLe$^x$, the signal darkening induced by iron oxide also seems to be greater than with USPIO, but not significantly ($p > 0.05$) (Fig. 5). The grafting of the sLe$^x$ mimetic, which contains a mannose residue, probably allows for an interaction of the USPIO with some molecules located at the surface of HUVECs. A slight uptake of USPIO-g-sLe$^x$ as compared to the ungrafted particles can therefore occur.

## MR imaging *in vivo*

Figure 7 shows the axial two-dimensional GE MR images resulting from USPIO-g-sLe$^x$ or USPIO injection to healthy and Con A-treated mice. In our model only hepatic failure is induced and no other organ is injured. Con A binds to endothelial cells of liver sinusoids and induces a T-cell mediated hepatitis (25, 26). E-selectin and other adhesion molecules are then massively expressed on the endothelium of liver vessels (27). A

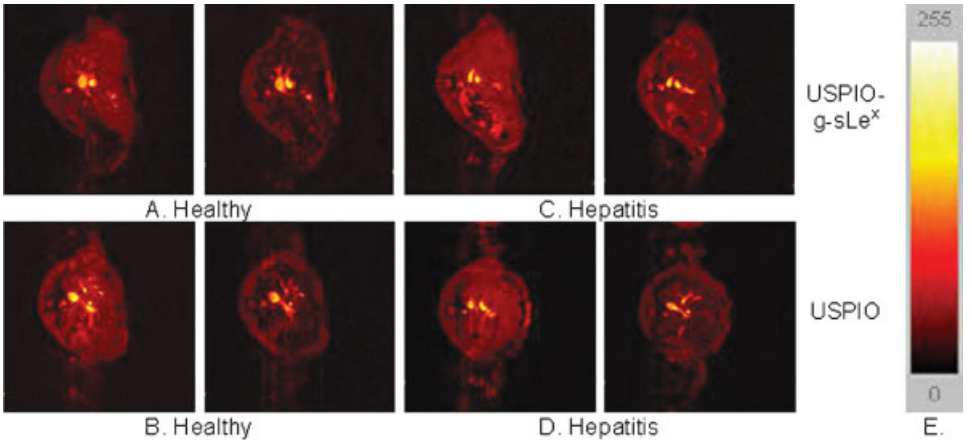


**Figure 7.** Axial GE MR images (TR/TE: 58.8/5.2 ms, FOV: 5.5 cm, matrix: $256 \times 256$, flip angle: 50°) of healthy (A, B) and Con A-treated (C, D) mice 65 min after the injection of 30 μmol Fe/kg of USPIO (B, D) or USPIO-g-sLe$^x$ (A, C). Color scale used for MR images signal intensities mapping with the Osiris software (E).

 

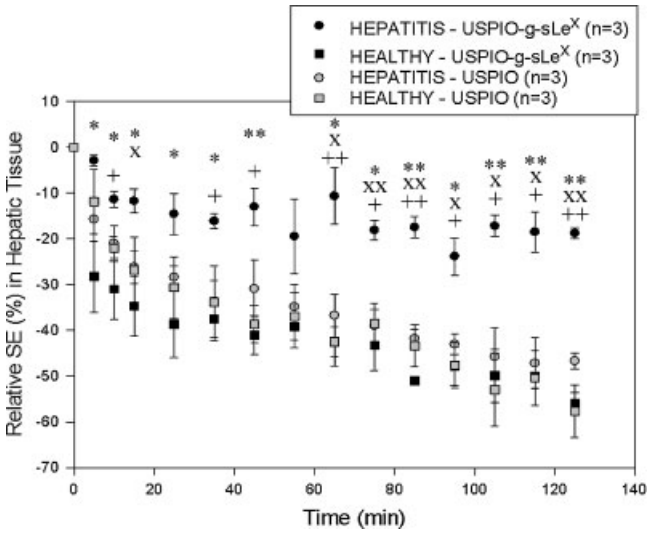


**Figure 8.** Relative signal intensity enhancement (SE) in the liver of healthy and ConA-treated mice after the injection of USPIO or USPIO-g-sLe$^X$. The results are represented as averages ± SEM and were statistically processed using Student's *t*-test: *: $P < 0.05$ and **: $P < 0.01$ as compared to healthy mice injected with USPIO-g-sLe$^X$, x: $P < 0.05$ and xx: $P < 0.01$ as compared to ConA-treated mice injected with USPIO, +: $P < 0.05$ and ++: $P < 0.01$ as compared to healthy mice injected with USPIO. (''n'' is the number of analyzed animals).

signal decrease, induced by the USPIO-g-sLe$^x$ or USPIO uptake, can be observed. However, with USPIO-g-sLe$^x$, the liver of the healthy mice becomes darker than that of the Con A-treated mice. This suggests that USPIO-g-sLe$^x$ are taken up by the Kupffer cells of diseased livers to a lesser extent, probably as a result of their interaction with E-selectin on the vascular endothelium.

Analysis of the MR images (Fig. 8) clearly shows that the relative signal enhancement (negative) measured in the liver of Con A-treated mice and injected with USPIO-g-sLe$^x$ is significantly larger than for the other groups after 1 h.

Particles of a size lower than 1000 nm can pass through the fenestrae of the liver sinusoids and are phagocyted by the Kupffer cells. USPIO are allowed to pass through the liver sinusoidal capillaries but, owing to their small size (20–40 nm), they are less well recognized by the Kupffer cells (28). Murine biodistribution studies, performed by MRI and microscopy, have shown that the cellular uptake of USPIO is negligible during the first hour after injection of doses similar to those used in this work, suggesting that the negative effect on signal intensity is predominantly due to USPIO remaining in the extracellular space. The capture of USPIO by the Kupffer cells peaking between 1 and 4 h post-injection, also contributes to the negative enhancement of signal intensity (29).

In our experiments, a difference between the liver signal intensity of Con A-treated mice injected with USPIO-g-sLe$^x$ and the liver signal intensity of the control groups can be observed immediately post-contrast, but only becomes significant in the second hour post-contrast. It could suggest that, at these time points, USPIO or USPIO-g-sLe$^x$ are at least partly in the intracellular compartment in the control groups, and that the largest part of USPIO-g-sLe$^x$ remains extracellular for a longer time in the Con A-treated group. These results can be explained by the fact that an interaction between USPIO-g-sLe$^x$ and the overexpressed endothelial E-selectin occurs in case of the Con A-induced liver inflammation, attenuating the extravasation of USPIO-g-sLe$^x$ in the liver parenchyma, and their uptake by Kupffer cells.

Kupffer cells dysfunction was invoked to explain the reduced hepatic uptake of small particles of iron oxide (SPIO), observed by MRI in patients with cirrhosis (30). Such a phenomenon can be excluded from our results since the uptake of USPIO is not significantly different between healthy and ConA-treated mice, suggesting that the function of Kuppfer cells is not altered by ConA.

After injection of USPIO-g-sLe$^x$, the relative signal enhancement of the hepatic tissue of healthy mice drops to significantly lower values than ConA-treated mice, even at the earliest time points, suggesting a faster uptake of the USPIO-g-sLe$^x$ by the healthy liver ($p < 0.05$ from 5 to 45 min post-injection). It is known that mannose or *N*-acetylglucosamine-terminated glycoproteins are quickly taken up by the liver thanks to a specific receptor located on sinusoidal cells (31). The mannose receptor (MR), a C-type surface lectin located at the surface of Kupffer cells and endothelial sinusoidal cells, could be responsible for a rapid capture of USPIO-g-sLe$^x$ because of the presence of a mannose residue in the sLe$^x$ mimetic molecule (32).

## CONCLUSIONS

The mimetic of the sialyl Lewis$^x$ has been grafted to USPIO, known as a powerful magnetic reporter. *In vitro* MR imaging performed on cell samples showed a higher retention of USPIO-g-sLe$^x$ by stimulated HUVECs, suggesting that an interaction occurs between the USPIO-g-sLe$^x$ and the E-selectins expressed at the surface of endothelial cells activated with TNF-$\alpha$.

*In vivo* results show that USPIO-g-sLe$^x$ has an interesting paradoxical potential for the *in vivo* diagnosis of inflammatory diseases. ConA-induced liver inflammation reduces the uptake of USPIO-g-sLe$^x$ by Kupffer cells. This unexpected situation is likely to be due to a retention of the specific contrast agent by E-selectin expressed on liver endothelial cells during inflammation. This observation is supported by the signal enhancement of the liver parenchyma. The blood half-life of USPIO is about 24 h in humans and 2 h in murine models. This latter value indicates the fact that USPIO are more easily taken up by liver macrophages in murine models (7). Nevertheless,

the decrease in the liver signal caused by the administration of USPIO-g-sLe$^x$ is significantly lower in ConA-treated mice, as compared to all the other cases.

These *in vivo* and *in vitro* MRI investigations both showed that the sLe$^x$ mimetic allows USPIO to interact with endothelial E-selectin, as demonstrated previously for the sLe$^x$ mimetic coupled to Gd-DTPA (19–21). The interest of superparamagnetic iron oxide nanoparticles as compared with the gadolinium-based contrast agents is their excellent detectability even at relatively low concentrations, which is relevant for molecular MRI applications. Leukocytes and endothelial cell adhesion molecules are becoming targets for the diagnosis of endothelial activation during inflammation, and for therapeutic interventions in diseases where an inflammatory process is implicated (33). The synthetic mimetic could also find applications in the therapeutic targeting of E-selectin, as it was achieved with an sLe$^x$ peptidomimetic (34, 35).

## Acknowledgements

The authors thank Professor Vincent Castronovo from the Metastasis Research Laboratory (University of Liège, Belgium) for providing the HUVECs and Professor Henri Alexandre from the Laboratory of Biology and Embryology (University of Mons-Hainaut, Belgium) for providing the mice.

## REFERENCES

1. Rennen HJ, Boerman OC, Oyen WJ, Corstens FH. Imaging infection/inflammation in the new millenium. *Eur. J. Nucl. Med*. 2001; **28**: 241–252.
2. Khatib AM, Kontogiannea M, Fallavollita L, Jamison B, Meterissian S, Brodt P. Rapid induction of cytokine and e-selectin expression in the liver in response to metastatic tumor cells. *Cancer Res*. 1999; **59**: 1356–1361.
3. Tanaka Y. The role of chemokines and adhesion molecules in the pathogenesis of rheumatoid arthritis. *Drugs Today (Barc)*. 2001; **37**: 477–484.
4. Menger MD, Vollmar B. Role of microcirculation in transplantation. *Microcirculation* 2000; **7**: 291–306.
5. Fan J, Watanabe T. Inflammatory reactions in the pathogenesis of atherosclerosis. *J. Atheroscler. Thromb*. 2003; **10**: 63–71.
6. Dousset V, Delalande C, Ballarino L, Quesson B, Seilhan D, Coussemacq M, Thiaudière E, Brochet B, Canioni P, Caillé JM. *In vivo* macrophage activity imaging in the central nervous system detected by magnetic resonance. *Magn. Reson. Med*. 1999; **41**: 329–333.
7. Dousset V, Gomez C, Petry KG, Delalande C, Caillé JM. Dose and scanning delay using USPIO for central nervous system macrophage imaging. *MAGMA* 1999; **8**: 185–189.
8. Dousset V, Doche B, Petry KG, Brochet B, Delalande C, Caillé JM. Correlation between clinical status and macrophage activity imaging in the central nervous system of rats. *Acad. Radiol*. 2002; **9** (Suppl. 1): S156–S159.
9. Fleige G, Nolte C, Synowitz M, Seeberger F, Kettenmann H, Zimmer C. Magnetic labeling of activated microglia in experimental gliomas. *Neoplasia* 2001; **3**: 489–499.
10. Rausch M, Hiestand P, Baumann D, Cannet C, Rudin M. MRI-based monitoring of inflammation and tissue damage in acute and chronic relapsing EAE. *Magn. Reson. Med*. 2003; **50**: 309–314.
11. Ruehm SG, Corot C, Vogt P, Kolb S, Debatin JF. Magnetic resonance imaging of atherosclerotic plaque with ultrasmall superparamagnetic particles of iron oxide in hyperlipidemic rabbits. *Circulation* 2001; **103**: 415–422.
12. Schoepf U, Marecos EM, Melder RJ, Jain RK, Weissleder R. Intracellular magnetic labeling of lymphocytes for *in vivo* trafficking studies. *Biotechniques* 1998; **24**: 642–651.
13. Anderson SA, Rader RK, Westlin WF, Null C, Jackson D, Lanza GM, Wickline SA, Kotyk JJ. Magnetic resonance contrast enhancement of neovasculature with alpha(v)beta(3)-targeted nanoparticles. *Magn. Reson. Med*. 2000; **44**: 433–439.
14. Bogdanov A, Matuszewski L, Bremer C, Petrovsky A, Weissleder R. Oligomerization of paramagnetic substrates result in signal amplification and can be used for MR imaging of molecular targets. *Mol. Imag*. 2002; **1**: 16–23.
15. Artemov D. Molecular magnetic resonance imaging with targeted contrast agents. *J. Cell Biochem*. 2003; **90**: 518–524.
16. Kang HW, Josephson L, Petrovsky A, Weissleder R, Bogdanov A Jr. Magnetic resonance imaging of inducible E-selectin expression in human endothelial cell culture. *Bioconjug. Chem*. 2002; **13**: 122–127.
17. Leeuwenberg JF, Smeets EF, Neefjes JJ, Shaffer MA, Cinek T, Jeunhomme TM, Ahern TJ, Buurman WA. E-selectin and intercellular adhesion molecule-1 are released by activated human endothelial cells *in vitro*. *Immunology* 1992; **77**: 543–549.
18. Fu Y, Laurent S, Muller RN. Synthesis of a sialyl Lewis X mimetic conjugated with DTPA, potential ligand of new contrast agents for medical imaging. *Eur. J. Org. Chem*. 2002; 3966–3973.
19. Sibson NR, Blamire AM, Bernades-Silva M, Laurent S, Boutry S, Muller RN, Styles P, Anthony DC. MRI detection of early endothelial activation in CNS inflammation. *Magn. Reson. Med*. 2004; **51**: 248–252.
20. Barber PA, Foniok T, Kick D, Buchan AM, Laurent S, Boutry S, Muller RN, Tuor UI. Magnetic resonance molecular imaging of early endothelial activation in focal cerebral ischemia in mice. *Ann. Neurol*. 2004; **56**: 116–120.
21. Boutry S, Burtea C, Laurent S, Toubeau G, Vander Elst L, Muller RN. Magnetic resonance imaging of inflammation with a specific selectin-targeted contrast agent. *Magn. Reson. Med*. 2005; **53**: 800–807.
22. Laurent S, Ouakssim A, Nicotra C, Gossuin Y, Roch A, Vander Elst L, Cornant M, Soleil P, Muller RN. Influence of the length of the coating molecules on the nuclear magnetic relaxivity of superparamagnetic colloids. *Phys. Stat. Sol. (c)* 2004; **1**: 3644–3650.
23. Terramani TT, Eton D, Bui PA, Wang Y, Weaver FA, Yu H. Human macrovascular endothelial cells: optimization of culture conditions. *In Vitro Cell Dev. Biol. Anim*. 2000; **36**: 125–132.
24. Seternes T, Sorensen K, Smedsrod B. Scavenger endothelial cells of vertebrates: A nonperipheral leukocyte system for high-capacity elimination of waste macromolecules. *Proc. Natl Acad. Sci. USA* 2002; **99**: 7594–7597.
25. Tiegs G, Hentschel J, Wendel A. A T cell-dependent experimental liver injury in mice inducible by concanavalin A. *J. Clin. Invest*. 1992; **90**: 196–203.
26. Tiegs G. Experimental hepatitis and role of cytokines. *Acta Gastroenterol. Belg*. 1997; **60**: 176–179.
27. Morikawa H, Hachiya K, Mizuhara H, Fujiwara H, Nishiguchi S, Shiomi S, Kuroki T, Kaneda K. Sublobular veins as the main site of lymphocyte adhesion/transmigration and adhesion molecule expression in the porto-sinusoidal—hepatic venous system during concanavalin a-induced hepatitis in mice. *Hepatology* 2000; **31**: 83–94.
28. Schuhmann-Giampieri G. Liver contrast media for magnetic resonance imaging. Interrelations between pharmacokinetics and imaging. *Invest Radiol*. 1993; **8**: 753–761.
29. Van Beers BE, Sempoux C, Materne R, Delos M, Smith AM. Biodistribution of ultrasmall iron oxide particles in the rat liver. *J. Magn. Reson. Imag*. 2001; **13**: 594–599.
30. Tanimoto A, Yuasa Y, Shinmoto H, Jinzaki M, Imai Y, Okuda S, Kuribayashi S. Superparamagnetic iron oxide-mediated hepatic signal intensity change in patients with and without cirrhosis: pulse

 

sequence effects and Kupffer cell function. *Radiology* 2002; **222**: 661–666.
31. Jansen RW, Molema G, Ching TL, Oosting R, Harms G, Moolenaar F, Hardonk MJ, Meijer DK. Hepatic endocytosis of various types of mannose-terminated albumins—what is important, sugar recognition, net charge, or the combination of these features. *J. Biol. Chem*. 1991; **266**: 3343–3348.
32. Feinberg H, Park-Snyder S, Kolatkar AR, Heise CT, Taylor ME, Weis WI. Structure of a C-type carbohydrate recognition domain from the macrophage mannose receptor. *J. Biol. Chem*. 2000; **275**: 21539–21548.
33. Ulbrich H, Eriksson EE, Lindbom L. Leukocyte and endothelial cell adhesion molecules as targets for therapeutic interventions in inflammatory disease. *Trends Pharmac. Sci*. 2003; **24**: 640–647.
34. Fukuda MN, Ohyama C, Lowitz K, Matsuo O, Pasqualini R, Ruoslahti E, Fukuda M. A peptide mimic of E-selectin ligand inhibits sialyl Lewis X-dependent lung colonization of tumor cells. *Cancer Res*. 2000; **60**: 450–456.
35. Renkonen R, Fukuda MN, Petrov L, Paavonen T, Renkonen J, Hayry P, Fukuda M. A peptide mimic of selectin ligands abolishes *in vivo* inflammation but has no effect on the rat heart allograft survival. *Transplantation* 2002; **74**: 2–6.

 